

# An Open-Source Mechanical Design of ALARIS Hand: A 6-DOF Anthropomorphic Robotic Hand

Ayaulym Nurpeissova, Talgat Tursynbekov and Almas Shintemirov, *Senior Member, IEEE*

**Abstract**—This paper presents a new open-source mechanical design of a 6-DOF anthropomorphic ALARIS robotic hand that can serve as a low-cost design platform for further customization and utilization for research and educational purposes. The presented hand design employs linkage-based three-phalange finger and two-phalange adaptive thumb designs with non-backdrivable worm-and-rack transmission mechanisms. Combination of design improvements and solutions, discussed in the paper, are implemented in a functional robotic hand prototype with powerful grasping capabilities, which utilizes off-the-shelf inexpensive components and 3D printing technology ensuring the hand low manufacturing cost and replicability. The open-source mechanical design of the presented ALARIS robotic hand is freely available for downloading from the authors' research lab web-site <https://www.alaris.kz> and [https://github.com/alarisnu/alaris\\_hand](https://github.com/alarisnu/alaris_hand).

## I. INTRODUCTION

Unlike industrial manipulators, service and humanoid robots are aimed to operate in unstructured and human environments executing variety of manipulation tasks with objects differing in size, shape and handling constraints. Human-shared environments are structured for easy manipulations of objects designed for humans, e.g. household items, tools, buttons, etc. [1], [2]. Mimicking human hand grasping patterns by anthropomorphic multi-fingered robotic hands remains one of the popular approaches to designing suitable highly articulated robotic grippers for service and humanoid robots as well as prosthetic hands with extended grasping capabilities.

Robotic hands can be differentiated by their finger design approaches. The use of fully actuated fingers ensures multiple degrees-of-freedom (DOF) and high dexterity of the designed robotic hands, e.g. [3], [4], which in turn, allows to perform fine object manipulation operations. On the other hand, such hand designs utilize large number of actuators, leading to increased number of sensing and actuation control loops, that results to overall high costs of the devices [1]. Tendon-driven underactuated finger actuation provides a design advantage that the finger actuating system can be placed outside the hand palm, thus allowing deployment of higher torque actuators [5]–[11]. On the other hand, tendon-driven mechanisms lead to complex coupled finger kinematics needed for accurate dexterous hand control [12] and may not be reliable in long-term usage due to tendon strengthening or wearing out [13].

This research was funded under the funded by the Kazakhstan Ministry of Education and Science's (project IRN AP08052091) and the Nazarbayev University (grant No.090118FD5340).

All authors are with the School of Engineering and Digital Sciences, Nazarbayev University, Nur-Sultan (Astana), Kazakhstan

A. Nurpeissova and T. Tursynbekov contributed equally to this work.

Corresponding author - A.Shintemirov, [ashintemirov@nu.edu.kz](mailto:ashintemirov@nu.edu.kz)

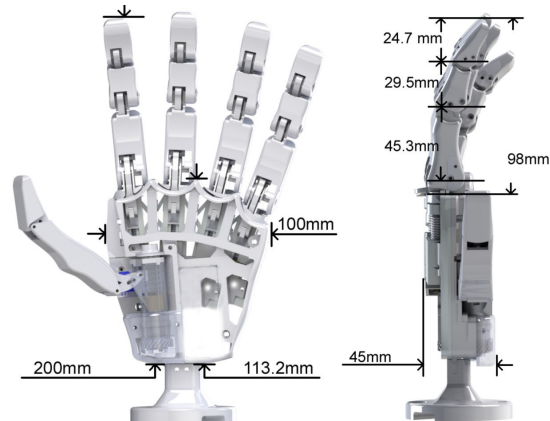


Fig. 1. ALARIS hand design with dimensions.

In contrast, a number of robotic and prosthetic hands have been proposed with underactuated finger designs based on mechanical linkage mechanisms, ensuring increased reliability and loading capacity. Since linkage mechanisms consist of rigid links and transmission gears, the finger and hand kinematics can be formulated as a standard kinematics problem for control purposes [14]–[16]. Prosthetic hands are usually designed with underactuated finger actuation through various differential drive mechanisms and simplified two-phalange finger designs [17]–[21]. On the other hand, robotic hands as well as linkage based industrial grippers normally ensure individual actuation of fingers with three-phalange structure for enhanced grasping performance, e.g. [22]–[26]. Such designs provide additional finger adaptation for enhanced object grasping and manipulation at the expense of complex dual actuation system and gear transmission, respectively, embodied within the palm and the finger bodies.

Commercially available dexterous robotic hands are normally very expensive in cost and do not allow extensive customisation of the design features for attachment to different robotic arm platforms or integration of additional sensors for research purposes [27]. To address such problems 3D printing rapid prototyping technology is actively applied for manufacturing of low-cost robotic hands that can be used in research and education [6]. This is facilitated through public release of open-source computer-aided design (CAD) models of robotic end-effectors that can be straightforwardly prototyped using low-cost 3D printers and assembled with use of off-the-shelf components, e.g. [15], [18], [27], [28].

To extend the choice of robotic hand designs freely available to robotics and prosthetics researchers, in this

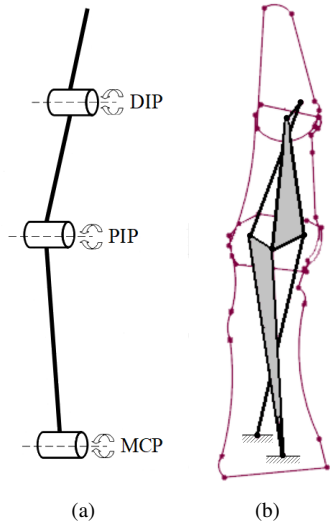


Fig. 2. Hand finger joints (a), a system (b) of coupled four-bar linkages of the finger mechanism.

paper the authors present a novel open-source mechanical design of a 6-DOF anthropomorphic robotic hand (Fig. 1). The proposed ALARIS hand design utilizes linkage-based three-phalange finger and two-phalange adaptive thumb designs with non-backdrivable worm-and-rack transmission mechanisms resulting to low-cost hand prototype demonstrating satisfactory object grasping performance. We also report various mechanical and hardware issues encountered and solved during the hand design process. The proposed open-source mechanical design of the robotic hand has been created using SolidWorks CAD software and is freely available for downloading from the authors' research lab web-site <https://www.alaris.kz> and [https://github.com/alarisnu/alaris\\_hand](https://github.com/alarisnu/alaris_hand), so it can serve as a low-cost design platform for further customization and utilization for research and educational purposes.

The paper is organized as follows. Section II briefly outlines the robotic hand design requirements, while Section III presents hand finger and thumb kinematic structures. The robotic hand design and its proof-of-concept prototype are then presented in Section IV, while the hand grasping performance is experientially evaluated in Section V. Conclusion section summarizes the main contributions of the paper.

## II. ROBOTIC HAND DESIGN REQUIREMENTS

Several design requirements were emphasised for designing the proposed anthropomorphic robotic hand: the hand and fingers should be able to perform standard prehensile postures, i.e. spherical, cylindrical (power), hook, lateral, tip [10], [18], and independent motion of each fingers for facilitating hand control research activities. Aiming to develop a simple hand design, a six DOF hand architecture was adopted for executing standard prehensile postures, with four identical in-line placed finger modules and one opposable thumb attached to a palm frame. Each of four in-line placed fingers is actuated by one motor providing 1-DOF mobility, whereas the

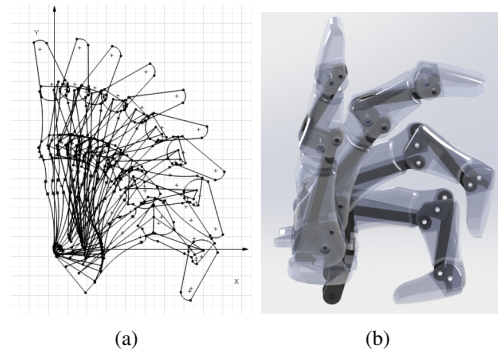


Fig. 3. Hand fingertip trajectory and finger workspace.

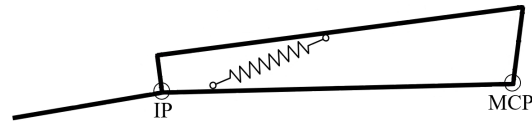


Fig. 4. Schematic model of the underactuated hand thumb.

thumb has 2-DOFs provided by 2 actuators for performing flexion/extension and axial rotation. The hand finger was designed to ensure hand anthropomorphic motion, appropriate geometrical dimensions and a simple mechanical system. The hand dimensions were chosen to be comparable with an average human male hand as presented in Fig. 1.

The requirement for an overall low cost of the hand was the another factor that justified many design choices. As the cost of finger actuators constitutes the largest part, identical off-the-shelf low-cost miniature brushed DC motors with integrated gearbox for higher torque output were utilized in the presented proof-of-concept hand design prototype. The hand design CAD files will be made publicly available for straightforward prototyping using any low cost 3D printer, which would eliminate the need for expensive, labor-intensive fabrication processes and facilitate the widespread use of the presented hand design in research and education applications. Additionally, by being open-source, the hand is fully customizable and, thus, could be modified for specific needs. For instance, the finger and thumb mechanisms can be redesigned to accommodate more reliable and accurate miniature servomotors for advanced hand motion control implementations.

## III. HAND FINGER AND THUMB KINEMATICS

### A. Hand Fingers

For design simplicity the presented ALARIS robotic hand utilizes four identical finger modules with each finger designed as a further evolution of the preliminary work [14]. Each hand finger provides 1-DOF motion. The proposed finger design consists of three phalanges (the distal phalange (DP), the middle phalange (MP), the proximal phalange (PP) as shown in Fig. 5) combined using four-bar linkage mechanisms to couple the finger distal interphalangeal (DIP), the proximal interphalangeal (PIP) and the metacarpal phalangeal (MCP) joints as schematically shown in Fig. 2. The

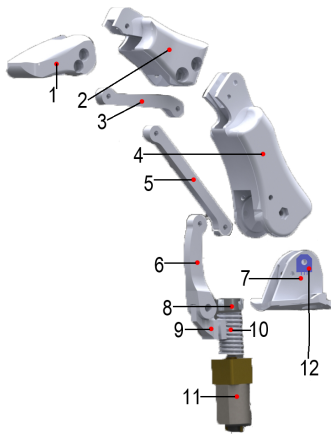


Fig. 5. Exploded view of the hand finger module: (1) distal phalange (DP); (2) middle phalange (MP); (3) link; (4) proximal phalange (PP); (5) link; (6) link; (7) finger base; (8) bearing; (9) rack; (10) worm gear; (11) DC motor; (12) position sensor.

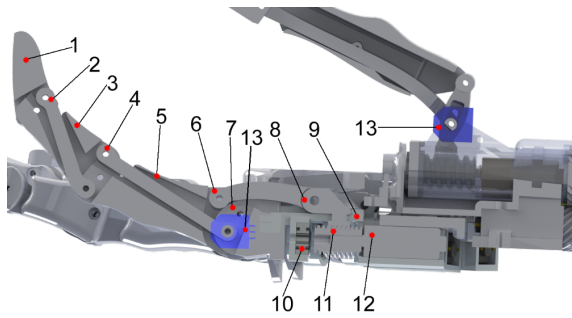


Fig. 6. Finger linkage and transmission design: (1) distal phalange (DP); (2) link; (3) middle phalange (MP); (4) link; (5) proximal phalange (PP); (6) link; (7) finger base; (8) rack; (9) navigating rail; (10) bearing; (11) worm gear; (12) DC motor; (13) position sensor.

abduction/adduction mobility at the finger MCP joint are excluded for ensuring hand design simplicity. The finger motion analysis was conducted using the vector-loop-closure mathematical model for a coupled system of two four-bar linkages of the finger mechanism presented in [14].

The finger linkage geometry was optimized using the SolidWorks' Sketch Blocks, the widely used tool for in planar mechanism design. The simulated fingertip trajectory and the finger workspaces for different final design finger postures starting from the straight finger until the closed grip position are demonstrated in Figure 3. A comparative analysis of the simulated final design fingertip path and the finger workspace with a typical human finger [29] on the same scale showed close convergence.

### B. Hand Thumb

The hand thumb is designed using a linkage-based adaptive finger design approach [30], previously adopted by the authors in [15] for an open-source adaptive robotic gripper design. Adaptive gripper finger designs ensured stable grasping of various shape objects due passive finger flexibility and

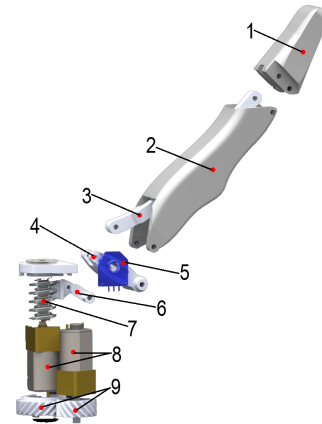


Fig. 7. Exploded view of the hand thumb module: (1) distal phalange (DP); (2) proximal phalange (PP); (3) link; (4) link; (5) position sensor; (6) rack; (7) worm; (8) DC motors; (9) helical gear of the thumb axial rotation.

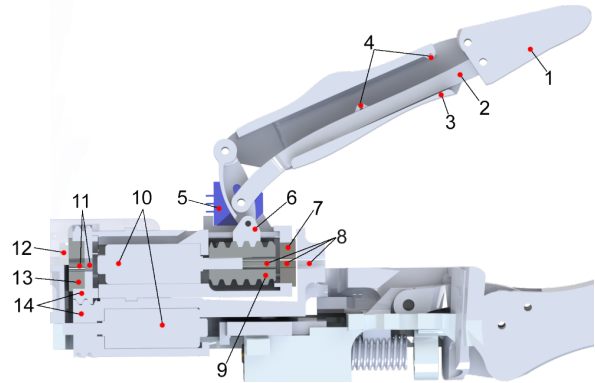


Fig. 8. Thumb linkage and transmission design: (1) distal phalange (DP); (2) link; (3) proximal phalange (PP); (4) spring holes; (5) position sensor; (6) rack; (7) bearing; (8) shaft; (9) worm; (10) DC motors; (11) shaft; (12) bearing; (13) bearing; (14) helical gear of the thumb axial rotation.

adaptivity between the thumb DOFs. Fig. 4 presents the 2-DOF linkage kinematics of the hand thumb with an actuated metacarpal phalangeal (MCP) joint and a passive element, i.e. a spring, within the thumb proximal phalange for transferring actuation from MCP to an interphalangeal (IP) joint, i.e. the thumb's second DOF. The spring's stiffness coefficient can be theoretically defined using the quasi-static equilibrium modelling of a two-phalange underactuated finger presented in [15]. However, in practice an appropriate spring for the thumb mechanism can be selected using a trial-and-error approach.

## IV. ROBOTIC HAND DESIGN

### A. Hand Actuation Mechanisms

The hand fingers and thumb are actuated by miniature DC motors with integrator gearbox (gear ratio 1:100). Initial experimentation with the finger actuation was performed using a ball screws for converting the rotation motion of an actuator into a linear motion of the driving finger linkage. However, initial tests revealed that this type of connection had generated vibration and caused disengagement of the bolt

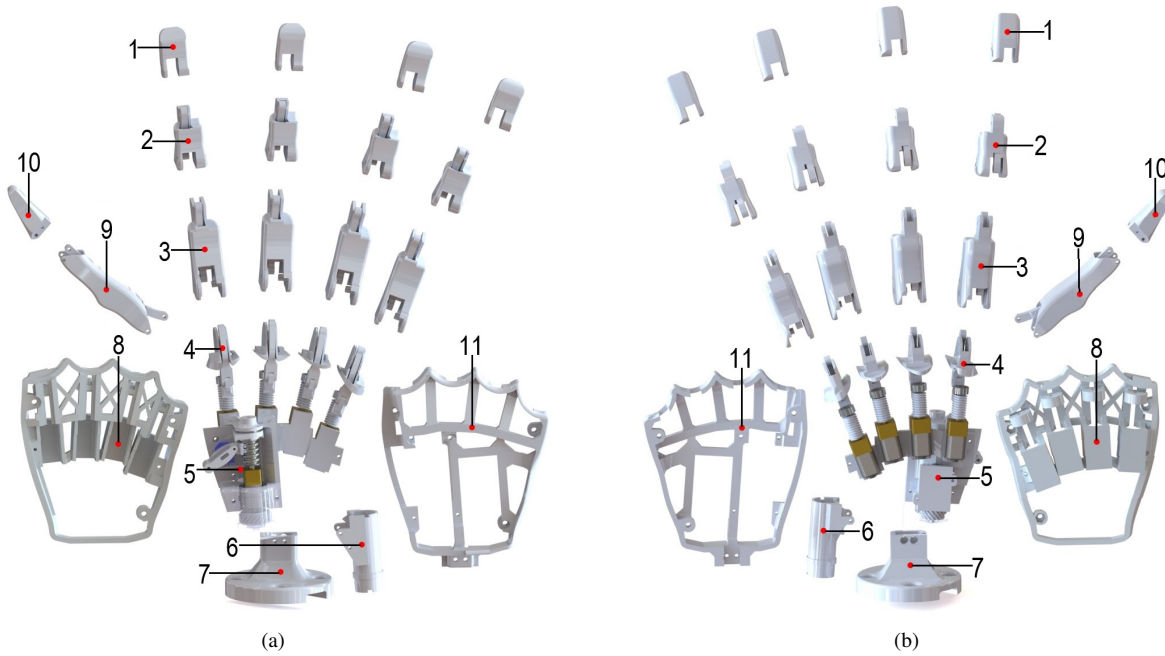


Fig. 9. Exploded view of ALARIS Hand: (a) front and (b) back views, where (1) distal phalange (DP); (2) middle phalange (MP); (3) proximal phalange (PP); (4) finger base; (5) thumb actuation system; (6) DC motor cover plate; (7) hand base; (8) back palm frame; (9) thumb proximal phalange (PP); (10) thumb distal phalange (DP); (11) front palm frame.

from the motor shaft. Therefore, additional navigation rails, guiding the finger and thumb driving links, were designed to eliminate vibrations in the finger transmission mechanisms. Although the vibration of the bolt decreased, it transferred to the nut, being rigidly connected to the output shaft of the motor. As a result, the vibration on the output motor shaft caused damaging of the actuator's built-in gearbox. Ultimately, it was decided to replace the ball screws with a worm-and-rack mechanisms in the final finger and thumb actuation modules. Along with solving the vibration problem, the worm-and-rack transmission makes the hand a non-backdrivable system, which ensures constant object grasping while the hand actuators are being powered-off.

Figures 5 and 6 present the complete finger module design consisting of the finger links, phalanges and transmission mechanism in the exploded assembly and cross-section views, respectively. Rotation of the worm gear attached to an actuator's shaft is converted to translation motion of the rack link moving along a navigating rail embedded in the hand back palm frame. The rack link is connected to a finger bar linkage, which folds the hand finger.

Figures 7 and 8 present the exploded assembly and cross-section views, respectively, of the thumb mechanism employing similar worm-and-rack transmission coupling. The thumb transmission module consists of 2-DOF joint, realized with a mechanical system of two motors, a worm-and-rack train, and a helical gear train. One actuator is fixed in the thumb transmission module (the upper DC motor in Fig. 8) and is responsible for the thumb's flexion/extension motions through the worm-and-rack transmission. The second actuator is located in the inside palm frame holder and provides axial

rotation of the thumb module through a helical gear.

The gear ratio of the finger worm-and-rack mechanism is defined based on the DC motor characteristics. The motor output shaft rotates at 150 rev/min with 0.35 kg/cm torque. The radius of the worm gear is 4.5 mm and pitch length per revolution is 1.5 mm. Substituting the data into a known worm-and-gear ration calculation expression the following value is obtained:

$$R = \frac{v_i}{v_o} = \frac{\omega \cdot r}{P/N \cdot N/sec} = \frac{2 \cdot \pi \cdot 4.5 \text{ mm}}{3.0 \text{ mm}/1} = 9.425, \quad (1)$$

where  $R$  - gear ratio,  $P$  - pitch,  $N$  - revolution,  $sec$  - second.

The gear ratio of the thumb worm-and-rack transmission mechanism is calculated with the same formula using the pitch length per revolution equal to 3.141 mm and the radius of worm gear equal to 5.5 mm.

$$R = \frac{v_i}{v_o} = \frac{2 \cdot \pi \cdot 5.5 \text{ mm}}{3.141 \text{ mm}/1} = 11. \quad (2)$$

The finger and thumb modules are designed to embed off-the-shelf resistive potentiometer sensors for implementing finger and thumb position controls. The finger potentiometer is aligned with the finger MCP joint and is fixed in a special niche inside the proximal phalange as shown in Fig. 6, whereas the thumb potentiometer is aligned with the thumb base joint (MCP joint in Fig. 4) and is fixed to the thumb base as shown in Fig. 8.

### B. Hand Prototype

The finger and thumb actuation modules are attached to two, i.e. front and back, hand palm frames, designed with navigating rails for finger worm-and-rack transmission mechanisms

TABLE I  
SPECIFICATION OF ALARIS ROBOTIC HAND

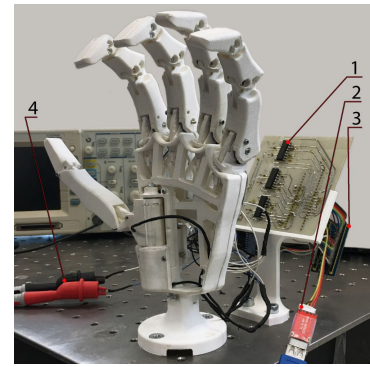
Parameter	Value
Dimensions	200x100x45 mm
Weight	413 g
Number of fingers	5
Number of actuators	6
Degrees of freedom	6
Average fingertip force	10N
Closing time	880ms
Opening time	880ms
Type of actuator	DC Brushed motor
Gear ratio of the DC motor gearbox	1:100
Operational current	150mA
Torque of motor	34.3 mN·m

TABLE II  
BILL OF MATERIALS OF ALARIS ROBOTIC HAND

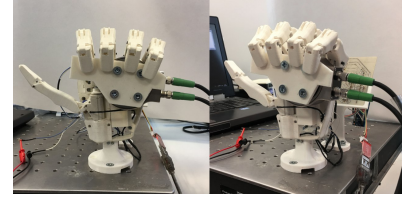
Parameter	Source	Quantity	Cost (USD)
Position sensor		6	36
DC Motor		6	101
Base	3D printed	1	12
Palm	3D printed	2	23
Distal interphalangeal joint (DIP)	3D printed	4	22
Proximal interphalangeal joint (PIP)	3D printed	4	28
Metacarpophalangeal joints (MCP)	3D printed	4	35
Thumb distal phalange (DP)	3D printed	1	11
Thumb proximal phalange (PP)	3D printed	1	13
Finger link	3D printed	12	27
Thumb link	3D printed	1	9
Finger base	3D printed	4	24
Bearing		7	17
Rack	3D printed	5	14
Worm gear	3D printed	5	32
Spring		9	23
Helical gear	3D printed	1	11
Screw and bolts		(approx.) 55	21
Wires and connectors		(approx.) 2m	19
Total			478

and cross structures for increased palm stiffness as shown in Fig. 9 in the exploded assembly views. The assembled hand design with geometric dimensions is illustrated in Fig. 1. At present, there are no palm covers designed for the presented hand design. The final palm cover shape would depend on dimensions of the hand embedded control system. Therefore, the authors leave the tasks of designing the hand palm cover and the embedded control system open for customization by interested researchers.

Figure 10(a) presents a proof-of-concept ALARIS robotic hand prototype, that was manufactured using a 3D printing technology with polylactide (PLA) material. The 3D printed parts of the hand are connected to each other by off-the-shelf 2.5 mm bolts and nuts, embedded to the special niches. The longer bolts are also used as finger and thumb joint shafts.

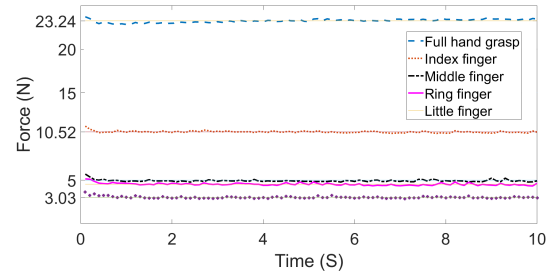


(a)

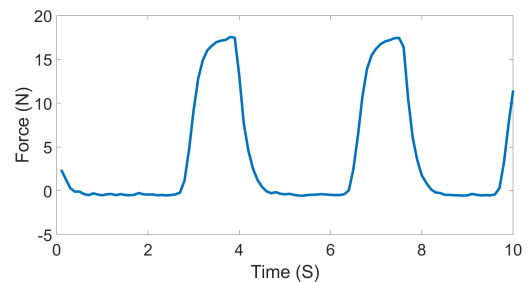


(b)

Fig. 10. ALARIS robotic hand prototype: (1) PCB; (2) USB to TTL for STM32; (3) STM32 control unit (4) Power supply alligator wires (a); Full hand grasping force measurements (b).



(a)



(b)

Fig. 11. Full grasp of ALARIS hand: (a) with separate output finger forces; (b) periodical grasping.

The hand prototype is rigidly mounted in a vertical position on a circular shape base holder to a laboratory optical plate. The holder can be easily replaced or redesigned for hand mounting on a robotic arm or a prosthesis socket. The power supply and control of the hand DC actuators is realized externally through L293D motor drivers mounted on a separate customly designed PCB board. The board also

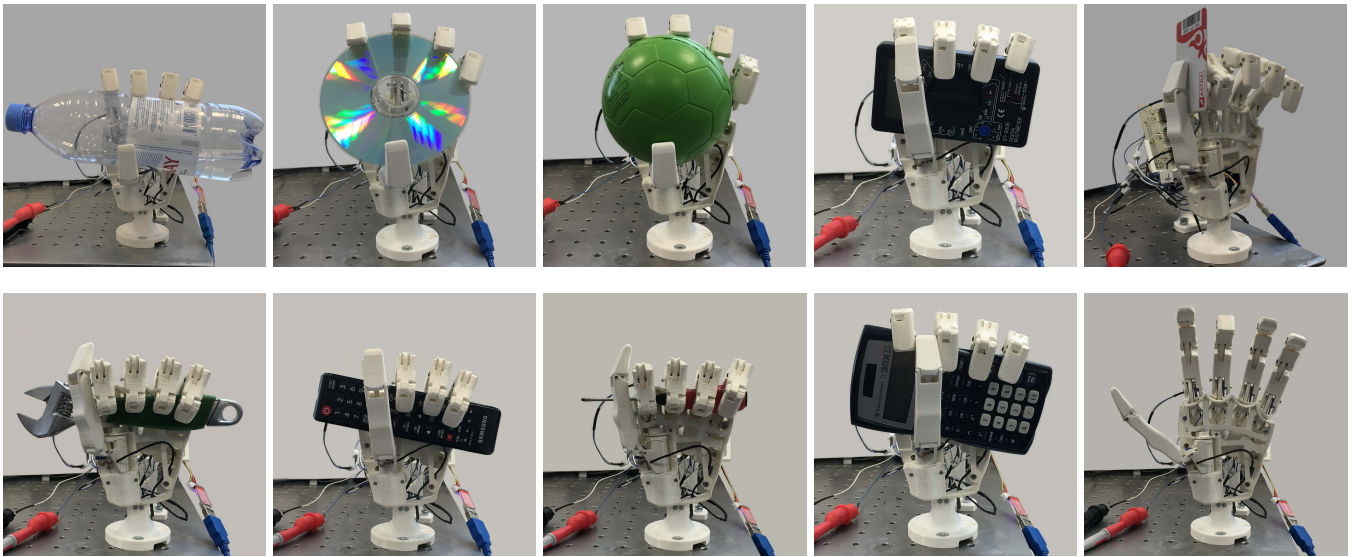


Fig. 12. Object grasp postures of ALARIS robotic hand while holding various objects.

houses a STM32 microcontroller for PWM control of the hand actuators using feedback signals from the hand built-in finger and thumb position potentiometers. Table I summarizes technical specifications, whereas Table II outlines the bill of materials and estimated cost of the presented ALARIS robotic hand prototype. Actuator, screws and nuts and standoff are commercially available at various robotics hobby/electronic and mechanical component distributors' web-sites and can be easily purchased. The overall cost of manufacturing the presented hand design without its embedded systems is estimated to be around 480 USD, assuming 40 USD cost estimate of 1 kg of PLA plastic used for 3D part printing.

## V. ROBOTIC HAND GRASPING PERFORMANCE

### A. Measurement Methodology

Evaluation of grasping performance of the developed 6-DOF ALARIS robotic hand started with experimental measurements of the forces exerted by the hand prototype. A Weiss Robotics KMS40 6-DOF force/torque sensor was utilized as a main measurement tool in the experiments. Force measurements were conducted to account only forces acting in  $Z$ -axis with the lowest value being recorded out of an array of forces measured within several consecutive test trials. Figure 10(b) demonstrates the grasping force measurement setups for the hand grasping force measurements using a specially designed pad for fixing the force sensor on the hand palm.

### B. Object Grasping Performance

The anthropomorphic ALARIS robotic hand was designed such that the thumb can oppose and reach the hand index, middle and ring fingers. The thumb opposition was evaluated using the Kapanji test [31], which assesses the capability of the thumb tip to touch different positions of the hand using a 0-10 point scale. According to the Kapanji test the designed ALARIS hand scored 4, which is a good result taking into

account the limited number of DOFs, i.e. 6, the robotic hand can employ comparing to 27 DOFs of a human hand.

The performance of the robotic hand was tested on grasping a variety of objects with different shapes, i.e. disc shaped, cylindrical, spherical and brick shaped items as demonstrated in Fig. 12. Based on the numerous trials and observations it is verified that hand can securely hold all objects. It was confirmed that the proposed underactuated adaptive thumb contributed effectively to reliable object envelopment during power grasping.

## VI. CONCLUSION

In this paper, a new open-source mechanical design of a 6-DOF anthropomorphic ALARIS robotic hand is presented to extend the choice of robotic hand designs freely available to robotics and prosthetics researchers. Combination of design improvements and solutions presented and discussed in the paper are implemented in a functional robotic hand prototype with powerful grasping capabilities, which utilizes off-the-shelf inexpensive components and 3D printing technology ensuring the hand low manufacturing cost and replicability. The robotic hand was experimentally tested with variety of objects in grasping tasks and output force measurements that demonstrated its feasibility for utilization in robotic research and teaching applications. The proposed open-source mechanical design of the robotic hand is freely available for downloading from the authors' research lab web-site <https://www.alaris.kz> and [https://github.com/alarisnu/alaris\\_hand](https://github.com/alarisnu/alaris_hand), so it can serve as a low-cost design platform for further customization and utilization in research and education applications.

## ACKNOWLEDGMENT

The authors would like to thank Mr. Nurdos Omarkulov, Mr. Kuat Telegenov and Ms. Bota Duisenbay for their contributions to preliminary robot hand design work.

## REFERENCES

- [1] T. Wiste and M. Goldfarb, "Design of a simplified compliant anthropomorphic robot hand," in *2017 IEEE International Conference on Robotics and Automation (ICRA)*, 2017, pp. 3433–3438.
- [2] S. W. Ruehl, C. Parlitz, G. Heppner, A. Hermann, A. Roennau, and R. Dillmann, "Experimental evaluation of the Schunk 5-Finger gripping hand for grasping tasks," in *2014 IEEE International Conference on Robotics and Biomimetics (ROBIO 2014)*, 2014, pp. 2465–2470.
- [3] H. Kawasaki, T. Komatsu, and K. Uchiyama, "Dexterous anthropomorphic robot hand with distributed tactile sensor: Gifu hand II," *IEEE/ASME Transactions on Mechatronics*, vol. 7, no. 3, pp. 296–303, 2002.
- [4] D. Lee, J. Park, S. Park, M. Baeg, and J. Bae, "KITECH-Hand: A highly dexterous and modularized robotic hand," *IEEE/ASME Transactions on Mechatronics*, vol. 22, no. 2, pp. 876–887, 2017.
- [5] T. Takaki and T. Omata, "High-performance anthropomorphic robot hand with grasping-force-magnification mechanism," *IEEE/ASME Transactions on Mechatronics*, vol. 16, no. 3, pp. 583–591, 2011.
- [6] Z. Kappassov, Y. Khassanov, A. Saudabayev, A. Shintemirov, and H. A. Varol, "Semi-anthropomorphic 3D printed multigrasp hand for industrial and service robots," in *Proceedings of the IEEE International Conference on Mechatronics and Automation (ICMA 2013)*, 2013, pp. 1697–1702.
- [7] K. Kim, S. H. Jeong, P. Kim, and K. Kim, "Design of robot hand with pneumatic dual-mode actuation mechanism powered by chemical gas generation method," *IEEE Robotics and Automation Letters*, vol. 3, no. 4, pp. 4193–4200, 2018.
- [8] S. H. Jeong, K.-S. Kim, and S. Kim, "Designing anthropomorphic robot hand with active dual-mode twisted string actuation mechanism and tiny tension sensors," *IEEE Robotics and Automation Letters*, vol. 2, no. 3, pp. 1571–1578, 2017.
- [9] "Shadow Robot Dexterous Hand," <https://www.shadowrobot.com/products/dexterous-hand/>.
- [10] D. Bennett, S. A. Dalley, D. Truex, and M. Goldfarb, "A multi-grasp hand prosthesis for providing precision and conformal grasps," *IEEE/ASME Transactions on Mechatronics*, vol. 20, no. 4, pp. 1697–1704, 2015.
- [11] H. Mnyusiwalla, P. Vulliez, J.-P. Gazeau, and S. Zeghloul, "A new dexterous hand based on bio-inspired finger design for inside-hand manipulation," *IEEE Transactions on Systems, Man, and Cybernetics: Systems*, vol. 46, no. 6, pp. 809–817, 2016.
- [12] Y.-T. Lee, H.-R. Choi, W.-K. Chung, and Y. Youm, "Stiffness control of a coupled tendon-driven robot hand," *IEEE Control Systems*, vol. 14, no. 5, pp. 10–19, 1994.
- [13] V. N. Dubey and R. M. Crowder, "A robotic finger mechanism for robust industrial applications," *Industrial Robot: An International Journal*, vol. 38, no. 4, pp. 352–360, 2011.
- [14] N. Omарkulov, K. Telegenov, M. Zeinullin, A. Begalinova, and A. Shintemirov, "Design and analysis of an underactuated anthropomorphic finger for upper limb prosthetics," in *2015 37th Annual International Conference of the IEEE Engineering in Medicine and Biology Society (EMBC)*, 2015, pp. 2474–2477.
- [15] K. Telegenov, Y. Tlegenov, and A. Shintemirov, "A low-cost open-source 3-D-printed three-finger gripper platform for research and educational purposes," *IEEE Access*, vol. 3, pp. 638–647, 2015.
- [16] H. Park and D. Kim, "An open-source anthropomorphic robot hand system: HRI hand," *HardwareX*, vol. 7, 2020.
- [17] P. Slade, A. Akhtar, M. Nguyen, and T. Bretl, "Tact: Design and performance of an open-source, affordable, myoelectric prosthetic hand," *2015 IEEE International Conference on Robotics and Automation (ICRA)*, pp. 6451–6456, 2015.
- [18] N. Krausz, R. Rorrer, and R. Weir, "Design and fabrication of a six degree-of-freedom open source hand," *IEEE Transactions on Neural Systems and Rehabilitation Engineering*, vol. 24, no. 5, pp. 562–572, 2016.
- [19] M. Controzzi, F. Clemente, D. Barone, A. Ghionzoli, and C. Cipriani, "The SSSA-MyHand a dexterous lightweight myoelectric hand prosthesis," *IEEE Transactions on Neural Systems and Rehabilitation Engineering*, vol. 25, no. 5, pp. 1571–1578, 2017.
- [20] "Bebionic Hand," <https://www.ottobockus.com/prosthetics/upper-limb-prosthetics/solution-overview/bebionic-hand/>.
- [21] J. Belter, J. Segil, A. Dollar, and R. Weir, "Mechanical design and performance specifications of anthropomorphic prosthetic hands: a review," *Journal of Rehabilitation Research and Development*, vol. 50, no. 5, pp. 599–618, 2013.
- [22] G. Cerruti, D. Chablat, D. Gouaillier, and S. Sakka, "ALPHA: A hybrid self-adaptable hand for a social humanoid robot," *2016 IEEE/RSJ International Conference on Intelligent Robots and Systems (IROS)*, vol. 20, no. 4, pp. 900–906, October 9-14, 2016.
- [23] J. Ueda, M. Kondo, and T. Ogasawara, "The multifingered NAIST hand system for robot in-hand manipulation," *Mechanism and Machine Theory*, vol. 45, no. 2, pp. 224–238, 2010.
- [24] "Robotiq 3-Finger Adaptive Robot Gripper," <https://robotiq.com/products/3-finger-adaptive-robot-gripper>.
- [25] L. U. Odhner and *et. al.*, "A compliant, underactuated hand for robust manipulation," *The International Journal of Robotics Research*, vol. 22(5), 2014.
- [26] C. Cipriani, M. Controzzi, and M. C. Carrozza, "The SmartHand transradial prosthesis," *Journal of NeuroEngineering and Rehabilitation*, 2011.
- [27] R. Ma, L. Odhner, and A. Dollar, "A modular, open-source 3D printed underactuated hand," in *Proceedings of the 2013 IEEE International Conference on Robotics and Automation (ICRA)*, 2013, pp. 2737–2743.
- [28] C. Piazza, G. Grioli, M. G. Catalano, and A. Bicchi, "A century of robotic hands," *Annual Review of Control, Robotics, and Autonomous Systems*, vol. 2, 2019.
- [29] D. G. Kamper, E. G. Cruz, and M. P. Siegel, "Stereotypical fingertip trajectories during grasp," *Journal of Neurophysiology*, vol. 90, no. 6, pp. 3702–3710, 2003.
- [30] L. Birglen and C. Gosselin, "Geometric design of three-phalanx underactuated fingers," *ASME Journal of Mechanical Design*, vol. 128, no. 2, pp. 356–364, 2005.
- [31] A. Kapandji, "Clinical test of apposition and counter-apposition of the thumb," *Annales de Chirurgie de la Main*, vol. 5, no. 1, pp. 67–73, 1986.